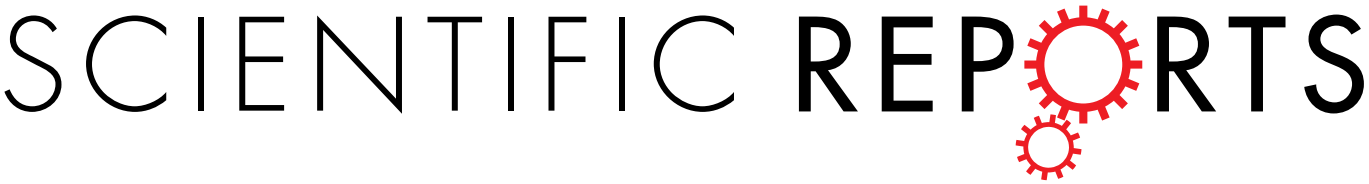

OPEN

Received: 21 July 2016
Accepted: 06 December 2016
Published: 19 January 2017

Predicting Drug Combination Index and Simulating the Network-Regulation Dynamics by Mathematical Modeling of Drug-Targeted EGFR-ERK Signaling Pathway

Lu Huang[1,2,3], Yuyang Jiang[1] & Yuzong Chen[3,4]

Synergistic drug combinations enable enhanced therapeutics. Their discovery typically involves the measurement and assessment of drug combination index (CI), which can be facilitated by the development and applications of in-silico CI predictive tools. In this work, we developed and tested the ability of a mathematical model of drug-targeted EGFR-ERK pathway in predicting CIs and in analyzing multiple synergistic drug combinations against observations. Our mathematical model was validated against the literature reported signaling, drug response dynamics, and EGFR-MEK drug combination effect. The predicted CIs and combination therapeutic effects of the EGFR-BRaf, BRaf-MEK, FTI-MEK, and FTI-BRaf inhibitor combinations showed consistent synergism. Our results suggest that existing pathway models may be potentially extended for developing drug-targeted pathway models to predict drug combination CI values, isobolograms, and drug-response surfaces as well as to analyze the dynamics of individual and combinations of drugs. With our model, the efficacy of potential drug combinations can be predicted. Our method complements the developed in-silico methods (e.g. the chemogenomic profile and the statistically-inferenced network models) by predicting drug combination effects from the perspectives of pathway dynamics using experimental or validated molecular kinetic constants, thereby facilitating the collective prediction of drug combination effects in diverse ranges of disease systems.

Synergistic drug combinations have been extensively explored for enhanced therapeutic efficacies[1–9]. In discovering and investigating synergistic drug combinations, the level of synergism is typically measured and quantified by the drug combination index (CI, a quantitative measure of drug combination effects defined in Method Section) such as Chou and Talalay's CI from experimental dose-response data[1,3,10]. Based on our literature search study, over 523 papers since 2004 have reported the discovery and optimization of synergistic drug combinations based on the experimentally determined CIs. In-silico tools that can predict CIs without the time-consuming and costly measurement of dose-response data are highly useful for facilitating the discovery of synergistic drug combinations.

[1]The Ministry-Province Jointly Constructed Base for State Key Lab and Shenzhen Technology and Engineering Lab for Personalized Cancer Diagnostics and Therapeutics Tsinghua University Shenzhen Graduate School, and Shenzhen Kivita Innovative Drug Discovery Institute, Shenzhen, 518055, P.R. China. [2]Institute of Molecular Biology (IMB), Ackermannweg 4, 55128 Mainz, Germany. [3]Department of Pharmacy, and Center for Computational Science and Engineering, National University of Singapore, Blk S16, Level 8, 3 Science Drive 2, 117543 Singapore. [4]State Key Laboratory of Biotherapy, West China Hospital, West China School of Medicine, Sichuan University, Chengdu, China. Correspondence and requests for materials should be addressed to Y.J. (email: jiangyy@sz.tsinghua.edu.cn) or Y.C. (email: phacyz@nus.edu.sg)

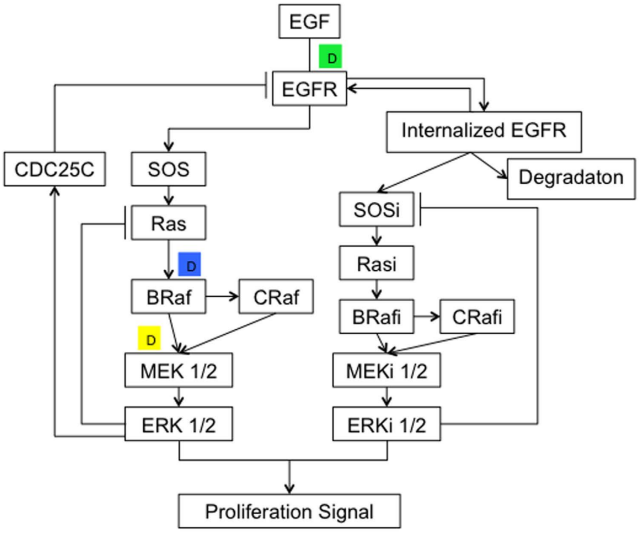

Figure 1. Drug-targeted EGFR-ERK pathway schema in this study. The EGFR, Raf and MEK inhibitor is represented by the small green, blue and yellow colored node with a letter D respectively.

Computational methods have been developed for predicting drug combination effects from gene expression profiles of drug-treated samples[11–15] and simulation of drug-targeted signaling[16–21] and metabolic[22–25] pathways. In particular, simulation of drug-targeted pathways is potentially useful for predicting CIs[17,26], as demonstrated by the successful applications of the chemogenomic profile based models[27,28] and the statistically-inferenced network models[29,30] for the prediction of synergistic effects of drug combinations. But the ability of the pathway simulation methods in predicting CIs has not been adequately tested against the observed values of multiple drug combinations targeting multiple target combinations. More tests are needed for determining what the existing mathematical models are capable of and what need to be further improved. These also provide useful knowledge for developing drug or drug combination targeted mathematical models for a number of pathways targeted by drugs and drug combinations (e.g. EGFR-ERK[31–35], apoptosis[36,37], NFκB[16,17], Wnt[19] and disease-relevant metabolic[22–25] pathways).

In this work, we developed and tested a mathematical model of drug and drug combination targeted EGFR-ERK pathway (Fig. 1) based on the ordinary differential equation model of Hornberg[38]. The method for developing this model is provided in the method section. This pathway was selected for two reasons. First, several kinases in this pathway have been targeted by individual inhibitor drugs and drug combinations with available experimental drug response and CI data[39–44]. Secondly, it is one of the pathways with well-established mathematical models[31–35,38], ideal for developing and testing drug-targeted pathway mathematical models. The kinase inhibitor drugs included in our mathematical model are EGFR, BRaf and MEK inhibitors, which together with their combinations have been clinically used or tested for the treatment of melanoma, colon, gastric, pancreatic, non-small-cell-lung-cancer (NSCLC) and other cancers[39–44].

The inhibitory effect of each drug against its target was measured by the percentage reduction of the integrated non-drug-bound target level at different drug concentrations (target dose response curve), and the concentration that induces 50% reduction was taken as the half maximal inhibitory concentration (IC50 value). The integrated non-drug-bound target level refers to the integral of the free target level over the first 2 hours of signaling stimulation. The anti-proliferative effect of each drug or drug combination was measured by the percentage reduction of the integrated phosphorylated ERK (ppERK) level (described below) with respect to the concentration(s) of the drug or drug combination (anti-proliferative dose effect curve)[45], and the concentration(s) that induce 90% reduction was taken as the half maximal inhibition of growth (GI50 value) of the drug or drug combination (details in the Method Section). The integrated ppERK level refers to the integral of the ppERK level over the first 2 hours of signaling stimulation (the ppERK level typically returns to the basal level <2 hours after HGF stimulation[46]). The anti-proliferative effect of a drug or drug combination was measured by its induced reduction of the integrated ppERK level for the following reason: The level of cell proliferation is linked to DNA synthesis, which is positively associated with the level of the integrated ERK2 activity[47], while the latter is correlated to the integrated ppERK level. However, a nonlinear correlation between the integrated ERK activity and cell proliferation rates is observed, with significant reduction of proliferation typically occurs when the ppERK level falls below 10% of its peak value[48,49]. Therefore, the concentration(s) of a drug or drug combination that induces 90% reduction of the integrated ppERK level was used to measure the GI50 value.

Our mathematical model was validated against the previously observed and simulated effects of the regulation of EGF, PP2A, MKP3 on ERK activities and the regulation of EGF on RasGTP, and its predicted anti-proliferate effects of EGFR, BRaf and MEK inhibitors were compared to the experimental cancer cell-line growth inhibition GI50 values. Additionally, the simulated efficiency of EGFR-MEK combination inhibitors was consistent with experimental results. It was then used to predict the effects of the combinations of EGFR-BRaf and BRaf-MEK inhibitors, and the computed anti-proliferate dose-effect curves were used to derive the drug-combination

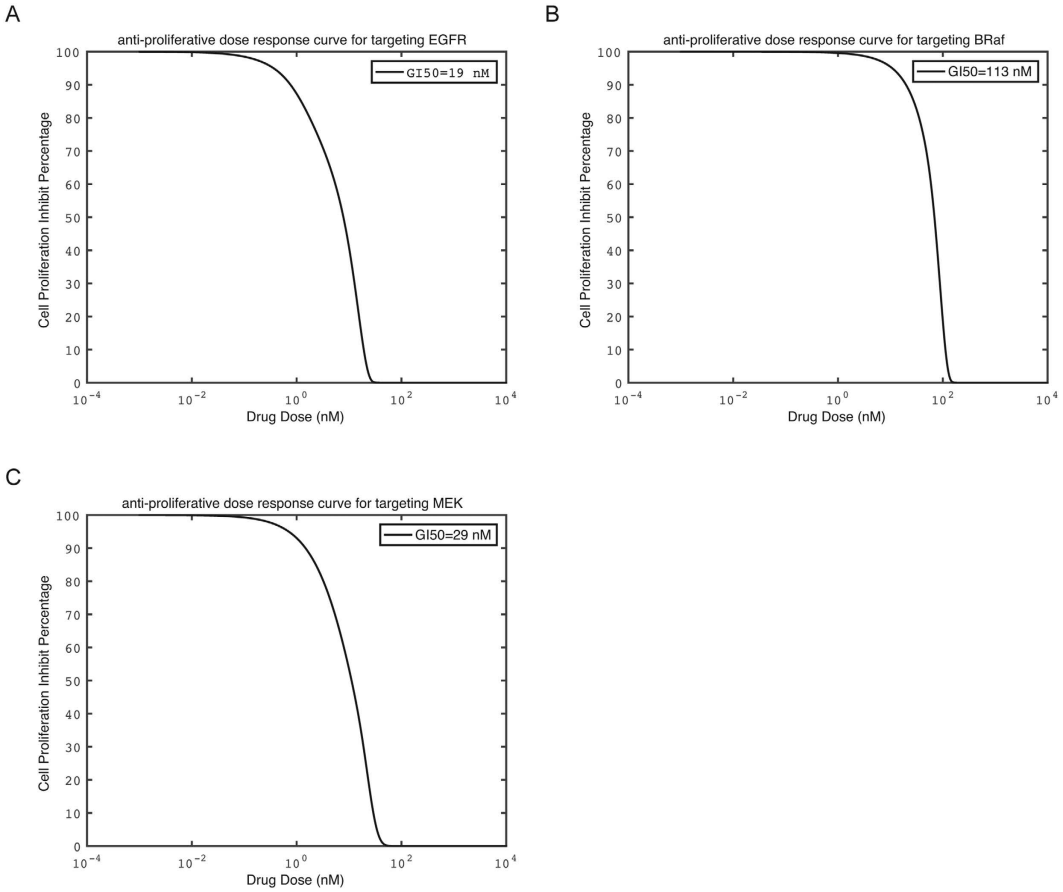

Figure 2. The computed anti-proliferative dose-response curve of individual inhibitors against EGFR-ERK pathway mediated cell growth signaling. (**A**) EGFR inhibitor; (**B**) BRaf inhibitor; (**C**) MEK inhibitor.

isobolograms and CIs based on Chou and Talalay's formula[10]. The predicted CIs were compared to the experimental values for evaluating the performance of the model.

Results and Discussions

Model validation against the observed signaling dynamics and the reported simulation results in the absence of a drug. Our mathematical model, described in the Method section, was first validated by comparing the simulated signaling dynamics in the absence of drugs with the literature-reported observations and simulation results. We found that the simulated time-dependent protein concentration profiles are in reasonable agreement with the experimentally determined profiles and the reported simulation results. At 8 nM EGF, the simulated ERK activation peaks within 5 minutes and decays within 2 hours (Supplementary Figure S1), which is consistent with the observed[46] and the simulated[38] ERK phosphorylation kinetics. The amount of simulated active RasGTP peaks at ~2 minutes and quickly decays within 10 minutes (Supplementary Figure S2), which is consistent with the observation that active RasGTP level in EGF- treated PC12 cells increases dramatically within 5 minutes and decays steeply within 10 minutes[32]. In simulating the regulation of EGFR-ERK signaling by phosphatases, we found that increasing PP2A level from 30000 to 60000 molecules/cell induces little changes in the peak amplitude but significantly reduces the duration of ERK activation (Supplementary Figure S3), while increasing MKP3 level from 9×10^6 to 1.5×10^7 molecules/cell significantly alters the peak amplitude and substantially reduces the duration of ERK activation (Supplementary Figure S4), which are consistent with the results of a reported simulation study showing that the duration of ERK activation is sensitive only to phosphatase reactions on MEK whereas the amplitude is most sensitive to phosphatase reactions on ERK[50].

Model validation against the experimental anti-proliferation activities of individual drugs. Our mathematical model was further validated by the comparison of the predicted GI50 values of individual EGFR, BRaf and MEK inhibitor with the reportedly observed GI50 values of known inhibitors against different cancer cell-lines[51,52]. Figure 2 shows the computed anti-proliferative dose-response curves of the EGFR, BRaf and MEK inhibitor respectively, and the computed target inhibitory dose-effect curves of these three inhibitors are shown in Supplementary Figures S5–S7 respectively. From Fig. 2, the computed GI50 values for EGFR, BRaf and MEK inhibitor are 19, 113, 29 nM respectively, which are within 10 fold of the largest experimental GI values against the cancer cell-lines promoted by the EGFR pathway (45 and 53 nM for EGFR inhibitor gefitinib and

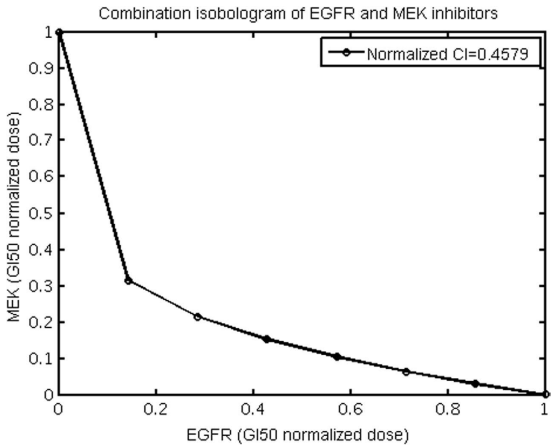

Figure 3. The computed isobologram for the combination of EGFR-MEK inhibitors.

erlotinib against non-small-cell lung cancer (NSCLC) cell-lines[51], 1.1 μM for BRaf inhibitor sorafenib against NSCLC cell-lines[50], and 14–200 nM for MEK inhibitor AZD6244 against thyroid cancer and melanoma cell lines[52].

The Kd values of the EGFR, BRaf and MEK inhibitors were set such that it gives the median IC50 (10 nM, 30 nM, and 15 nM for EGFR, BRaf, MEK inhibitors respectively) corresponding to the highly potent IC50 values of the drugs frequently used in pharmaceutical research (12.5 ± 7.5 nM against EGFR, 28 ± 3 nM against BRaf, and 15.5 ± 3.5 nM against MEK, details in the Method Section). The predicted GI50 values of the EGFR and MEK inhibitors are substantially smaller than (by 4–6 fold) that of the BRaf inhibitor. This is consistent with the observed behavior of the highly potent inhibitors with the largest experimental GI values (by 5.5–22 fold) against the cancer cell-lines promoted by the EGFR pathway. Analysis of the interaction dynamics of our mathematical model (Fig. 1) suggested that this phenomenon arises from the additional bypass signaling through BRaf-CRaf dimers after BRaf inhibitor binding to BRaf. As a result, increasing activity of the BRaf inhibitor stimulates the bypass signaling mediated through CRaf, and vice versa, leading to an overall less efficient anti-proliferative effect by the BRaf inhibitor than that by the EGFR and MEK inhibitor respectively.

Our mathematical model, was derived from the conventional models[31–35,38] and drug-target binding kinetics[34] with the parameters fitted to the median IC50 values of potent inhibitors. Variation of the IC50 from 5 nM to 50 nM led to comparable degree of variations in the predicted GI50 values (9–95 nM, 19–195 nM and 10–99 nM for EGFR, BRaf and MEK inhibitor respectively). The consistency of the predicted and observed GI values suggests that our mathematical model may have some capability in facilitating the quantitative study of the anti-proliferative activities of the drugs and drug combinations targeting the EGFR pathway.

Model validation against the experimental anti-proliferation activities of EGFR-MEK inhibitors combination. We used our mathematical model to simulate the anti-proliferative effect and to compute the CI values of drug-pair EGFR-MEK inhibitors. As in the cases of drug combination studies[1,3,10], the concentration-dependent anti-proliferative effect of drug-pair was measured by an isobologram that displays a curve of the dose-combinations of the two drugs that produce 90% reduction of the integrated ppERK levels within the first 2 hours of signaling stimulation. Figure 3 shows the computed isobologram for the combination of EGFR-MEK inhibitors. The computed CI values for the combinations of EGFR-MEK is 0.46. These are comparable to the experimental values 0.4–0.8 for EGFR-MEK[40], which suggest that our mathematical model has some level of capability in facilitating the prediction of CI values.

Prediction of drug combination effects of EGFR-BRaf, BRaf-MEK. BRaf is a commonly mutated oncogene, yet there are no effective therapies exist for BRaf mutant cancers. Mostly because targeting BRaf or MEK kinase in BRaf mutant cancer, respectively, frequently activates other bypass pathways, thus constraining the effectiveness of these inhibitors as single-agents. In our mathematical model, we further predict the combination therapy strategies for BRaf mutant cancers with two drug combination effects, EGFR-BRaf and BRaf-MEK inhibitors, respectively. In modeling of these two drug-pairs, the same set of kinetic parameters for modeling as each individual drug was used. Figure 4 showed the computed isobolograms for the combination of EGFR-BRaf, BRaf-MEK inhibitors. The computed CI values for the combinations of EGFR-BRaf, and BRaf-MEK are 0.69 and 0.87, respectively.

The synergistic effects of these two drug combinations arise from the same type of synergistic mode of action: the complementary action involving positive regulation of a target by targeting two upstream-downstream points of a pathway[8,53,54]. For the EGFR-BRaf inhibitor combination, the inhibitory activity of the EGFR inhibitor reduces the activation BRaf to complement the inhibitory activity of the BRaf inhibitor. For the BRaf-MEK inhibitor combination, the inhibitory activity of BRaf reduces the activation of MEK to complement the inhibitory activity of MEK inhibitor. These two combinations have largely similar level of synergism as judged by the similar quantities of the computed and observed CI values, which is likely due to the same type of synergistic mode of action.

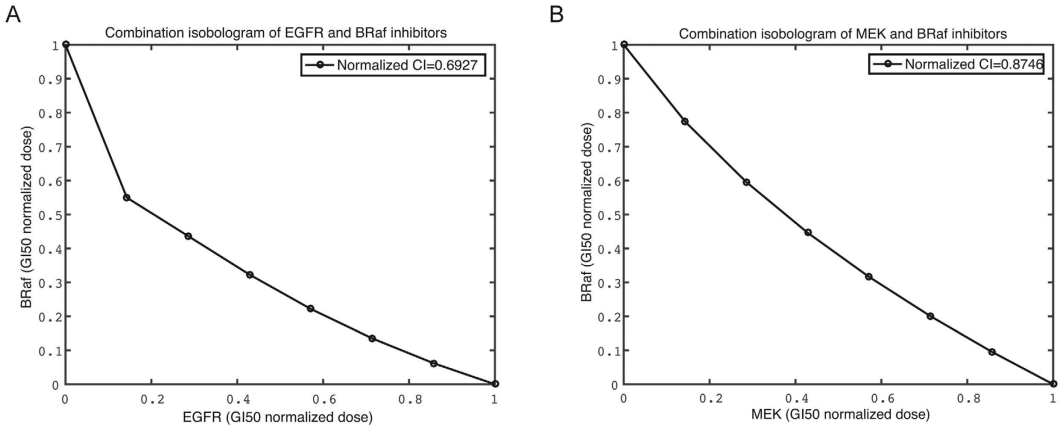

Figure 4. The predicted isobologram for two drug combinations. (**A**) EGFR-BRaf inhibitors; (**B**) BRaf-MEK inhibitors.

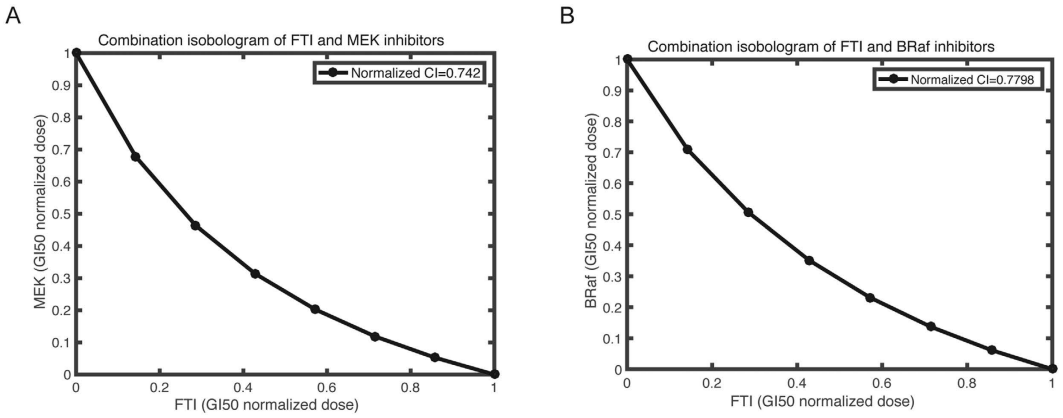

Figure 5. The predicted isobologram for combination treatment of farnesyltransferase inhibitors (FTIs) and drugs. (**A**) FTI-MEK inhibitor; (**B**) FTI-BRaf inhibitor.

Prediction of combination effects of a farnesyltransferase inhibitor combined with a drug targeting BRaf or MEK. Mutated *Ras* genes that produce constitutively active Ras proteins are found to be involved in approximately 30% of human cancers, including several pancreatic and colon carcinomas. Anticancer therapeutic development has been focusing on blockage of hyper-activation of Ras protein, e.g. through farnesyltransferase inhibitors (FTIs) which inhibit the farnesylation of RAS, preventing Ras transform into the functional form that can be attached to the cell-membrane and subsequently transmit signals to the Raf-MEK-ERK (MAPK) signaling pathways, which have a major role in melanoma progression[55]. However, FTIs alone is frequently insufficient for the treatment of cancers. In our mathematical model, we simulated the combination effects of two types of drug combinations, FTI-MEK and FTI-BRaf inhibitors, respectively. FTIs are modeled in our study as drugs inhibiting the transformation of RasGDP to functional RasGTP. The association and dissociation constants k_{on} and k_{off} for FTIs are optimized to give IC50 of 10 nM, since most FTIs in pharmaceutical research has less than 10 nM IC50 values[56,57].

Figure 5 showed the computed isobologram for the combination of FTI-MEK inhibitor, FTI-BRaf inhibitor. The computed CI values for the combinations of FTI-MEK inhibitor, and FTI-BRaf inhibitor are 0.74 and 0.78, respectively. The predicted synergism effects of these two drug combinations are consistent with recent literature report that combinations of lonafarnib (a specific FTI) with pan-RAF inhibitor sorafenib yielded additional growth-inhibiting effects than lonafarnib and sorafenib used alone[58]. Moreover, the apoptosis-inducing effect of BMS-214662 (another cytotoxic FTI) has been significantly enhanced through combination treatment with a MEK inhibitor, PD184352, leading to a complete suppression on invasive tumor growth in K562 and CD34 + CML cells[59]. Both our model and experimental studies suggest that the combination treatment of FTI and Raf and MEK-inhibitor may represent an effective alternative for melanoma treatment, and therefore worth further exploration.

Conclusions

Our drug-targeted EGFR-ERK pathway mathematical model, developed based on existing drug-free models and drug-target interaction kinetics, and validated against a number of published experimental and simulation results, showed fairly good potential in predicting the individual and combination drug effects on the cell-proliferation

signaling of the pathway. In particular, the predicted drug combination CI values are comparable to the experimental values for the combination of EGFR-BRaf, EGFR-MEK, BRaf-MEK, FTI-MEK, and FTI-Raf inhibitors[41], suggesting that existing pathway models may be potentially extended for developing drug-targeted pathway mathematical models to predict drug combination CI values, isobolograms, and drug-response surfaces/curves as well as to analyze the dynamics of individual and combination of drugs. Our model provides a strategy to predict efficacy of these MAPK pathway inhibitors through novel targeted therapy combination approaches.

Further development efforts are needed to explore drug-targeted pathway mathematical models as practical tools for facilitating the discovery of synergistic drug combinations. For instance, some synergistic drug combinations are known to arise from the activities against multiple pathways[8]. Although several multi-pathway models have been developed[60–62], there is a need to refine existing and develop more multi-pathway models to sufficiently cover the multiple pathways relevant to synergistic drug combinations. Moreover, in some cases, drug effects are influenced by pathway crosstalks[63,64], and drug actions at the multiple sites[65,66], states[67], conformations[1], and mutant forms[1] of the same target. There is a need to add these elements into the existing and newly developed pathway models for extended coverage of therapeutically relevant biological networks and the modes of actions of individual drugs and drug combinations[8].

Methods

Construction of Mathematical Model. Our pathway model schema is illustrated in Fig. 1. We based our model of EGFR signaling on that of Hornberg *et al.*, which itself is a refinement of earlier work. The components of drug-target interactions were added to the ordinary differential equation model of Hornberg *et al.*[38,68], with an additional ERK-CDC25C-EGFR feedback loop[44] and the interactions between BRaf and CRaf[69] incorporated. The model contains 126 distinct molecular species, and 190 elementary reactions; these reactions are described as a series of ordinary differential equations based on the mass action law. The model is parameterized by 123 kinetic parameters and 126 initial molecular concentrations. A typical enzyme catalyzed reaction in the pathway and the mass-action based rate is shown in the equations below, where the A and B represent species or concentration of species, depending on the context:

$$A + B \underset{K_f}{\overset{K_b}{\leftrightarrows}} [A{:}\ B]$$
$$\frac{dA}{dt} = K_b \cdot [A{:}\ B] - K_f \cdot A \cdot B \tag{1}$$

The rate equations are defined by the forward and reverse rate constants K_f and K_b or turnover K_{cat} used in the published models[31,32,38,70–73] or reported from other literatures. The constituent molecular interactions, their kinetic constants, and molecular concentrations are detailed in Supplementary Table S1. Fourth order Runge-Kutta method with adaptive step-size control was used for solving these equations.

Kinetic Parameters. The types of parameters used in our mathematical model are protein-protein interactions, drug-protein interactions, and catalytic activities. The published simulation studies have shown that most parameters are robust and insensitive to significantly alter the overall pathway behavior[31,32]. Apart from the use of the parameters of the published mathematical models, additional parameters were obtained from the literatures based on the widely used assumption that the parameters measured *in vitro* and in some cell lines are generally applicable in most cases. For those protein-protein interactions with unavailable parameters, their parameters were putatively estimated from the known parameters of the relevant interacting domain profile pairs[74,75] or other interacting protein pairs of similar sequences.

Drug targeting. Drugs targeting each component in the EGFR signaling pathway were simulated as forming complexes with target components based on the mass action law. These inhibitors include the individual EGFR, BRaf, MEK inhibitor or the combination of EGFR-MEK, EGFR-BRaf, and BRaf-MEK inhibitors respectively. For simulating the interaction between each drug and its target, we followed Bairy and Wong[34] to introduce an extra species, the drug, and two reactions to describe drug-target association and dissociation, with the corresponding kinetic constants K_{on} and K_{off} determined such that the K_{off} takes a value of 0.01 s^{-1}, while the K_{on} was determined such that the drug gives the median IC50 (10 nM, 30 nM, and 15 nM for EGFR, BRaf, MEK inhibitors respectively) corresponding to the highly potent IC50 values of the drugs frequently used in pharmaceutical research (Cetuximab 1 nM, Erlotinib 2 nM, Afatinib 14 nM and Gefitinib 33 nM against EGFR, Sorafenib 25 nM and Vemurafenib 31 nM against BRaf, and AZD6244 12 nM and RDEA119 19 nM against MEK).

$$\text{Drug} + \text{Target} \underset{K_{\text{on}}}{\overset{K_{\text{off}}}{\leftrightarrows}} [\text{Drug: Target}] \tag{2}$$

Definition of IC50 and GI50 values. IC50 is defined as the half maximal inhibitory concentration that induces 50% reduction of integrated non-drug-bound target level. The integrated non-drug-bound target level refers to the integral of the free target level over the first 2 hours of signaling stimulation. For the reasons described in the Introduction Section, the drug concentration-dependent (from 0.001 nM to 10 μM) effects on the ERK-mediated cell-growth signaling process were determined by measuring the percentage of ppERK reduction within the first 2 hours of signaling stimulation. GI50 is defined as the growth inhibition concentration that induces 90% reduction of ppERK within the first 2 hours. Further analysis showed that the variation of the GI50 values from 80% to 99% of ppERK reduction resulted in insignificant changes in the predicted CI values (±0.1),

and thus no changes in the qualitative conclusion of the synergistic or antagonistic levels of drug combinations. This indicates the robustness of our drug-binding models in predicting drug combination effects.

Computation of the combination index and isobolograms for quantitative determination of drug interactions. Quantifying drug interactions in drug combination studies and classifying the interactions into categories of synergy, additivity, or antagonism are of interest to many researchers. Isobologram and combination index (CI) analyses are widely used methods for evaluating drug interactions in combination cancer chemotherapy. The Loewe additivity model has been largely used as a reference model when the combined effect of two drugs is additive. The model can be written as in Equation (3):

$$\frac{(D)_1}{(Dx)_1} + \frac{(D)_2}{(Dx)_2} = 1 \tag{3}$$

where $(D)_1$ and $(D)_2$ are the respective combination doses of drug 1 and drug 2 that yield an effect of 50% growth inhibition, with $(D_x)_1$ and $(D_x)_2$ being the corresponding single doses for drug 1 and drug 2 that result in the same effect, which is by definition the GI50 of drug 1 and drug 2. When Eq. 3 holds, it can be concluded that the combined effect of the two drugs is additive. Based on Eq. 3, the combination index, defined in Eq. 4, can be used to classify drug interactions as synergistic, additive, or antagonistic.

$$CI = \frac{(D)_1}{(Dx)_1} + \frac{(D)_2}{(Dx)_2} \tag{4}$$

$$CI < 1 \text{ synergy;} \quad CI = 1 \text{ additivity;} \quad CI > 1 \text{ antagonism}$$

A CI of less than, equal to, and more than 1 indicates synergy, additivity, and antagonism, respectively.

We simulated isobolograms for a pair of drugs with eight equally effective dose combinations for a particular effect level of GI50. GI50 normalized doses of drug 1 and drug 2 that give this effect in combination are plotted as axial points in the isobologram graphs. According to Eq. 4, the isobologram curves are expected to be parallel to the diagonal for additive drug pairs, concave for synergistic drug pairs, and convex for antagonistic drug pairs. We mainly concerned about the qualitative shape of the isobolograms for correctly identifying the drug pair category, and use the smallest CI of the eight drug dose combinations as the CI for this drug pair.

References

1. Keith, C. T., Borisy, A. a. & Stockwell, B. R. Multicomponent therapeutics for networked systems. *Nat. Rev. Drug Discov.* **4,** 71–78 (2005).
2. Csermely, P., Agoston, V. & Pongor, S. The efficiency of multi-target drugs: The network approach might help drug design. *Trends in Pharmacological Sciences* **26,** 178–182 (2005).
3. Zimmermann, G. R., Lehar, J. & Keith, C. T. Multi-target therapeutics: when the whole is greater than the sum of the parts. *Drug Discovery Today* **12,** 34–42 (2007).
4. Smalley, K. S. M. *et al.* Multiple signaling pathways must be targeted to overcome drug resistance in cell lines derived from melanoma metastases. *Mol. Cancer Ther.* **5,** 1136–1144 (2006).
5. Dancey, J. E. & Chen, H. X. Strategies for optimizing combinations of molecularly targeted anticancer agents. *Nat. Rev. Drug Discov.* **5,** 649–659 (2006).
6. Kitano, H. A robustness-based approach to systems-oriented drug design. *Nat. Rev. Drug Discov.* **6,** 202–210 (2007).
7. Silver, L. L. Multi-targeting by monotherapeutic antibacterials. *Nat. Rev. Drug Discov.* **6,** 41–55 (2007).
8. Jia, J. *et al.* Mechanisms of drug combinations: interaction and network perspectives. *Nat. Rev. Drug Discov.* **8,** 111–128 (2009).
9. Hopkins, A. L. Network pharmacology: the next paradigm in drug discovery. *Nat. Chem. Biol.* **4,** 682–90 (2008).
10. Chou, T.-C. Theoretical basis, experimental design, and computerized simulation of synergism and antagonism in drug combination studies. *Pharmacol. Rev.* **58,** 621–81 (2006).
11. Cline, E. I., Bicciato, S., DiBello, C. & Lingen, M. W. Prediction of *in vivo* synergistic activity of antiangiogenic compounds by gene expression profiling. *Cancer Res.* **62,** 7143–7148 (2002).
12. Beerenwinkel, N. *et al.* Methods for optimizing antiviral combination therapies. In *Bioinformatics* **19** (2003).
13. Havaleshko, D. M. *et al.* Prediction of drug combination chemosensitivity in human bladder cancer. *Mol. Cancer Ther.* **6,** 578–586 (2007).
14. Small, B. G. *et al.* Efficient discovery of anti-inflammatory small-molecule combinations using evolutionary computing. *Nat. Chem. Biol.* **7,** 902–8 (2011).
15. Lee, J. H. *et al.* CDA: Combinatorial drug discovery using transcriptional response modules. *PLoS One* **7** (2012).
16. Yan, H., Zhang, B., Li, S. & Zhao, Q. A formal model for analyzing drug combination effects and its application in TNF-alpha-induced NFkappaB pathway. *BMC Syst. Biol.* **4,** 50 (2010).
17. Peng, H., Wen, J., Li, H., Chang, J. & Zhou, X. Drug inhibition profile prediction for NF??B pathway in multiple myeloma. *PLoS One* **6** (2011).
18. Al-Shyoukh, I. *et al.* Systematic quantitative characterization of cellular responses induced by multiple signals. *BMC Syst. Biol.* **5,** 88 (2011).
19. Kogan, Y. *et al.* A new validated mathematical model of the Wnt signalling pathway predicts effective combinational therapy by sFRP and Dkk. *Biochem. J.* **444,** 115–125 (2012).
20. Glants, R. M., Turchin, V. L., Chaplik, V. V. & Gribovich, IuIa. Treatment of acute renal insufficiency using prostaglandin E2 in surgical patients. *Klinicheskaia khirurgiia* 32–34 (1990).
21. Miller, M. L. *et al.* Drug synergy screen and network modeling in dedifferentiated liposarcoma identifies CDK4 and IGF1R as synergistic drug targets. *Sci. Signal.* **6,** ra85–ra85 (2013).
22. Lehár, J. *et al.* Chemical combination effects predict connectivity in biological systems. *Mol. Syst. Biol.* **3,** 80 (2007).
23. Yang, K. *et al.* Dynamic simulations on the arachidonic acid metabolic network. *PLoS Comput. Biol.* **3,** 0523–0530 (2007).
24. Buse, E. Generation of GABA-synthesizing nerve cells cultured from embryonic cortex cerebri of mice with and without cell-to-cell contacts. *Anat Embryol* **182,** 151–160 (1990).
25. Facchetti, G., Zampieri, M. & Altafini, C. Predicting and characterizing selective multiple drug treatments for metabolic diseases and cancer. *BMC Syst. Biol.* **6,** 115 (2012).

26. Sun, X. *et al.* Cytokine combination therapy prediction for bone remodeling in tissue engineering based on the intracellular signaling pathway. *Biomaterials* **33,** 8265–8276 (2012).
27. Jansen, G. *et al.* Chemogenomic profiling predicts antifungal synergies. *Mol. Syst. Biol.* **5,** 338 (2009).
28. Chandrasekaran, S. *et al.* Chemogenomics and orthology-based design of antibiotic combination therapies. *Mol. Syst. Biol.* **12,** 872 (2016).
29. Molinelli, E. J. *et al.* Perturbation Biology: Inferring Signaling Networks in Cellular Systems. *PLoS Comput. Biol.* **9** (2013).
30. Korkut, A. *et al.* Perturbation biology nominates upstream–downstream drug combinations in RAF inhibitor resistant melanoma cells. *Elife* **4** (2015).
31. Schoeberl, B., Eichler-Jonsson, C., Gilles, E. D. & Müller, G. Computational modeling of the dynamics of the MAP kinase cascade activated by surface and internalized EGF receptors. *Nat. Biotechnol.* **20,** 370–375 (2002).
32. Sasagawa, S., Ozaki, Y., Fujita, K. & Kuroda, S. Prediction and validation of the distinct dynamics of transient and sustained ERK activation. *Nat. Cell Biol.* **7,** 365–373 (2005).
33. Li, H. *et al.* Pathway sensitivity analysis for detecting pro-proliferation activities of oncogenes and tumor suppressors of epidermal growth factor receptor- extracellular signal-regulated protein kinase pathway at altered protein levels. *Cancer* **115,** 4246–4263 (2009).
34. Bairy, S. & Wong, C. F. Influence of kinetics of drug binding on EGFR signaling: A comparative study of three EGFR signaling pathway models. *Proteins Struct. Funct. Bioinforma.* **79,** 2491–2504 (2011).
35. Huang, L. *et al.* Simulating EGFR-ERK signaling control by scaffold proteins KSR and MP1 reveals differential Ligand-Sensitivity Co-Regulated by CBL-CIN85 and Endophilin. *PLoS One* **6** (2011).
36. Fussenegger, M., Bailey, J. E. & Varner, J. A mathematical model of caspase function in apoptosis. *Nat. Biotechnol.* **18,** 768–774 (2000).
37. Legewie, S., Blüthgen, N. & Herzel, H. Mathematical modeling identifies inhibitors of apoptosis as mediators of positive feedback and bistability. *PLoS Comput. Biol.* **2,** 1061–1073 (2006).
38. Hornberg, J. J. *et al.* Control of MAPK signalling: from complexity to what really matters. *Oncogene* **24,** 5533–5542 (2005).
39. Normanno, N. *et al.* The MEK/MAPK pathway is involved in the resistance of breast cancer cells to the EGFR tyrosine kinase inhibitor gefitinib. *J. Cell. Physiol.* **207,** 420–427 (2006).
40. Yoon, Y. K. *et al.* Combination of EGFR and MEK1/2 inhibitor shows synergistic effects by suppressing EGFR/HER3-dependent AKT activation in human gastric cancer cells. *Mol Cancer Ther* **8,** 2526–2536 (2009).
41. Martinelli, E. *et al.* Synergistic antitumor activity of sorafenib in combination with epidermal growth factor receptor inhibitors in colorectal and lung cancer cells. *Clin. Cancer Res.* **16,** 4990–5001 (2010).
42. Diep, C. H., Munoz, R. M., Choudhary, A., Von Hoff, D. D. & Han, H. Synergistic effect between erlotinib and MEK inhibitors in KRAS wild-type human pancreatic cancer cells. *Clin. Cancer Res.* **17,** 2744–2756 (2011).
43. Su, F. *et al.* Resistance to selective BRAF inhibition can be mediated by modest upstream pathway activation. *Cancer Res.* **72,** 969–978 (2012).
44. Prahallad, A. *et al.* Unresponsiveness of colon cancer to BRAF(V600E) inhibition through feedback activation of EGFR. *Nature* **483,** 100–3 (2012).
45. Klinger, B. *et al.* Network quantification of EGFR signaling unveils potential for targeted combination therapy. *Mol. Syst. Biol.* **9,** 673 (2013).
46. Hornberg, J. J., Tijssen, M. R. & Lankelma, J. Synergistic activation of signalling to extracellular signal-regulated kinases 1 and 2 by epidermal growth factor and 4 beta-phorbol 12-myristate 13-acetate. *Eur. J. Biochem.* **271,** 3905–13 (2004).
47. Asthagiri, a. R., Reinhart, C. a., Horwitz, a. F. & Lauffenburger, D. a. The role of transient ERK2 signals in fibronectin- and insulin-mediated DNA synthesis. *J. Cell Sci.* **113** Pt 24, 4499–4510 (2000).
48. Albeck, J. G., Mills, G. B. & Brugge, J. S. Frequency-Modulated Pulses of ERK Activity Transmit Quantitative Proliferation Signals. *Mol. Cell* **49,** 249–261 (2013).
49. Yang, H. *et al.* RG7204 (PLX4032), a selective BRAFV600E inhibitor, displays potent antitumor activity in preclinical melanoma models. *Cancer Res.* **70,** 5518–5527 (2010).
50. Mayawala, K., Gelmi, C. a. & Edwards, J. S. MAPK cascade possesses decoupled controllability of signal amplification and duration. *Biophys. J.* **87,** L01–L02 (2004).
51. Holbeck, S. L., Collins, J. M. & Doroshow, J. H. Analysis of Food and Drug Administration-Approved Anticancer Agents in the NCI60 Panel of Human Tumor Cell Lines. *Mol. Cancer Ther.* **9,** 1451–60 (2010).
52. Ball, D. W. *et al.* Selective growth inhibition in BRAF mutant thyroid cancer by the mitogen-activated protein kinase kinase 1/2 inhibitor AZD6244. *J. Clin. Endocrinol. Metab.* **92,** 4712–4718 (2007).
53. Dai, Z., Liu, S., Marcucci, G. & Sadee, W. 5-Aza-2′-deoxycytidine and depsipeptide synergistically induce expression of BIK (BCL2-interacting killer). *Biochem. Biophys. Res. Commun.* **351,** 455–461 (2006).
54. Georgakis, G. V., Li, Y., Rassidakis, G. Z., Medeiros, L. J. & Younes, A. The HSP90 inhibitor 17-AAG synergizes with doxorubicin and U0126 in anaplastic large cell lymphoma irrespective of ALK expression. *Exp. Hematol.* **34,** 1670–1679 (2006).
55. Rowinsky, E. K., Windle, J. J. & Von Hoff, D. D. Ras protein farnesyltransferase: A strategic target for anticancer therapeutic development. *J. Clin. Oncol.* **17,** 3631–3652 (1999).
56. Chaponis, D. *et al.* Lonafarnib (SCH66336) improves the activity of temozolomide and radiation for orthotopic malignant gliomas. *J. Neurooncol.* **104,** 179–189 (2011).
57. Basso, A. D. *et al.* The farnesyl transferase inhibitor (FTI) SCH66336 (lonafarnib) inhibits Rheb farnesylation and mTOR signaling: Role in FTI enhancement of taxane and tamoxifen anti-tumor activity. *J. Biol. Chem.* **280,** 31101–31108 (2005).
58. Niessner, H. *et al.* The farnesyl transferase inhibitor lonafarnib inhibits mTOR signaling and enforces sorafenib-induced apoptosis in melanoma cells. *J. Invest. Dermatol.* **131,** 468–479 (2011).
59. Pellicano, F. *et al.* The MEK inhibitor PD184352 enhances BMS-214662-induced apoptosis in CD34+CML stem/progenitor cells. *Leukemia* **25,** 1159–67 (2011).
60. Fisher, C. P., Plant, N. J., Moore, J. B., Kierzek, A. M. & Jurisica, I. QSSPN: Dynamic simulation of molecular interaction networks describing gene regulation, signalling and whole-cell metabolism in human cells. *Bioinformatics* **29,** 3181–3190 (2013).
61. Proctor, C. J., Macdonald, C., Milner, J. M., Rowan, A. D. & Cawston, T. E. A computer simulation approach to assessing therapeutic intervention points for the prevention of cytokine-induced cartilage breakdown. *Arthritis Rheumatol.* **66,** 979–989 (2014).
62. Gong, H. & Feng, L. Computational analysis of the roles of ER-Golgi network in the cell cycle. *BMC Syst. Biol.* **8,** S3 (2014).
63. Peng, X.-H. *et al.* Cross-talk between epidermal growth factor receptor and hypoxia-inducible factor-1alpha signal pathways increases resistance to apoptosis by up-regulating survivin gene expression. *J. Biol. Chem.* **281,** 25903–14 (2006).
64. Massarweh, S. & Schiff, R. Resistance to endocrine therapy in breast cancer: Exploiting estrogen receptor/growth factor signaling crosstalk. in *Endocrine-Related Cancer* **13** (2006).
65. Grimaldi, K. a., McAdam, S. R., Souhami, R. L. & Hartley, J. a. DNA damage by anti-cancer agents resolved at the nucleotide level of a single copy gene: evidence for a novel binding site for cisplatin in cells. *Nucleic Acids Res.* **22,** 2311–7 (1994).
66. Malonga, H., Neault, J. F., Diamantoglou, S. & Tajmir-Riahi, H. A. Taxol anticancer activity and DNA binding. *Mini Rev. Med. Chem.* **5,** 307–311 (2005).
67. Sintchak, M. D. *et al.* Structure and mechanism of inosine monophosphate dehydrogenase in complex with the immunosuppressant mycophenolic acid. *Cell* **85,** 921–930 (1996).

68. Apgar, J. F., Toettcher, J. E., Endy, D., White, F. M. & Tidor, B. Stimulus design for model selection and validation in cell signaling. *PLoS Comput. Biol.* **4** (2008).
69. Stites, E. C. The response of cancers to BRAF inhibition underscores the importance of cancer systems biology. *Sci. Signal.* **5,** pe46 (2012).
70. Zhang, B., Chernoff, J. & Zheng, Y. Interaction of Rac1 with GTPase-activating proteins and putative effectors. A comparison with Cdc42 and RhoA. *J. Biol. Chem.* **273,** 8776–8782 (1998).
71. Kholodenko, B. N., Demin, O. V., Moehren, G. & Hoek, J. B. Quantification of short term signaling by the epidermal growth factor receptor. *J. Biol. Chem.* **274,** 30169–30181 (1999).
72. Yamada, S., Taketomi, T. & Yoshimura, A. Model analysis of difference between EGF pathway and FGF pathway. *Biochem. Biophys. Res. Commun.* **314,** 1113–1120 (2004).
73. Kiyatkin, A. *et al.* Scaffolding protein Grb2-associated binder 1 sustains epidermal growth factor-induced mitogenic and survival signaling by multiple positive feedback loops. *J. Biol. Chem.* **281,** 19925–19938 (2006).
74. Wojcik, J. & Schächter, V. Protein-protein interaction map inference using interacting domain profile pairs. *Bioinformatics* **17** Suppl 1, S296–S305 (2001).
75. Singhal, M. & Resat, H. A domain-based approach to predict protein-protein interactions. *BMC Bioinformatics* **8,** 199 (2007).

Acknowledgements

This work is supported by Academic Research Fund (R-148-000-081-112/101) National University of Singapore.

Author Contributions

L.H. and Y.Z.C. conceived, designed the study and created the computational methods. L.H. performed the computational analysis. L.H., Y.Z.C. and Y.Y.J. analyzed the data and wrote the manuscript. All authors reviewed and commented on the manuscript.

Additional Information

Supplementary information accompanies this paper at http://www.nature.com/srep

Competing financial interests: The authors declare no competing financial interests.

How to cite this article: Huang, L. *et al.* Predicting Drug Combination Index and Simulating the Network-Regulation Dynamics by Mathematical Modeling of Drug-Targeted EGFR-ERK Signaling Pathway. *Sci. Rep.* **7**, 40752; doi: 10.1038/srep40752 (2017).

Publisher's note: Springer Nature remains neutral with regard to jurisdictional claims in published maps and institutional affiliations.